

## REPORT

## POLYMERS

# Semiconducting polymer blends that exhibit stable charge transport at high temperatures

Aristide Gumyusenge<sup>1</sup>, Dung T. Tran<sup>1</sup>, Xuyi Luo<sup>1</sup>, Gregory M. Pitch<sup>2</sup>, Yan Zhao<sup>1</sup>, Kaelon A. Jenkins<sup>1</sup>, Tim J. Dunn<sup>3</sup>, Alexander L. Ayzner<sup>2</sup>, Brett M. Savoie<sup>4\*</sup>, Jianguo Mei<sup>1\*</sup>

Although high-temperature operation (i.e., beyond 150°C) is of great interest for many electronics applications, achieving stable carrier mobilities for organic semiconductors at elevated temperatures is fundamentally challenging. We report a general strategy to make thermally stable high-temperature semiconducting polymer blends, composed of interpenetrating semicrystalline conjugated polymers and high glass-transition temperature insulating matrices. When properly engineered, such polymer blends display a temperature-insensitive charge transport behavior with hole mobility exceeding 2.0 cm<sup>2</sup>/V·s across a wide temperature range from room temperature up to 220°C in thin-film transistors.

The performance of inorganic semiconductors optimized for operation at ambient temperatures degrades at elevated temperatures. Charge carriers are thermally promoted across the band gap, which leads to increased carrier densities, junction leakages, and reduced charge carrier mobility (1–3). To improve the device performance and lifetime in these harsh thermal conditions, wide-bandgap materials have been utilized (4, 5). Alternatively, active or passive cooling, thermally engineered packaging, as well as electrical isolation between multiple transistors are used to maintain the optimal electronic performance (6). By contrast, organic semiconductors commonly display thermally activated charge transport features (7, 8). Charge transport is facilitated in organics with moderate temperature increases, leading to improved performance (9). However, this thermally activated charge transport becomes counteracted by unstable morphologies and disrupted molecular packing at higher temperatures, especially in polymer thin films (10, 11). Although devices

such as organic field-effect transistors are now common (12), their operation is normally at ambient conditions. High-temperature annealing effects have been explored in organic semiconductors (13–15), but in all reports, charge-carrier mobilities have been temperature dependent and start to decline at >150°C.

Blending semiconducting polymers with insulating hosts has been used as a general strategy to improve electronic performance, processability, and mechanical and environmental stability in electronic devices (16–18). Preserving close intermolecular interactions and packing motifs at elevated temperatures is the key challenge, especially for semiconducting polymers (10, 19). We hypothesized that interpenetrating networks between semicrystalline conjugated polymers and high glass-transition ( $T_g$ ) insulating polymers can confine conformational changes of semiconducting polymer chains at elevated temperatures. To test this concept, we first select diketopyrrolopyrrole-thiophene (DPP-T; P1), a high-performance conjugated polymer, and poly(N-vinyl carbazole) (PVK,  $T_g \sim 220^\circ\text{C}$ ) as the high- $T_g$  host (Fig. 1A) and studied blends from 40 to 90 weight % (wt %) of PVK in spin-cast films. The blends with between 55 and 65 wt % PVK formed interpenetrating channels between the conjugated polymer P1 and the rigid host PVK, as observed from atomic force microscopy (AFM) images (Fig. 1B and fig. S1).

Testing the blend films in field-effect transistors (FETs) under ambient and inert

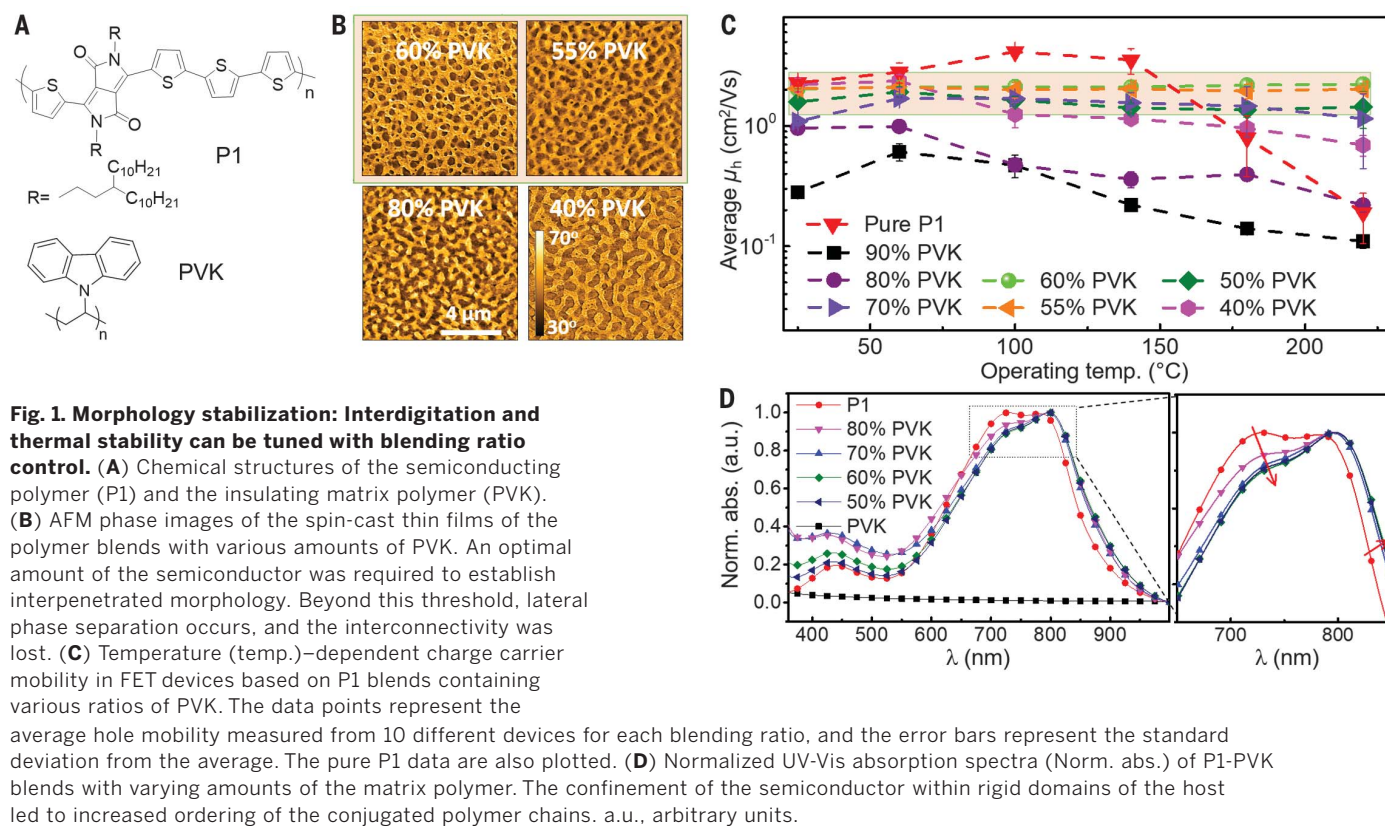
conditions, we observed thermally stable operations at high temperatures up to 220°C with hole mobilities as high as 2.5 cm<sup>2</sup>/V·s at the blend ratios of 55 to 65 wt % PVK that created a bicontinuous morphology with interconnected P1 domains (Fig. 1C and fig. S2). With loadings outside this range, undesired vertical or large lateral phase segregation occurs, which leads to the loss of thermal stability. The mobility of the pristine semiconductor P1 decreases to 8% at 220°C. Ultraviolet-visible (UV-Vis) absorption spectra (Fig. 1D) revealed an increase in the 0-0 vibronic peak intensities upon approaching the optimal blending ratios, indicative of increasing ordering and  $\pi$ - $\pi$  interactions between P1 chains in the confined domains (20–22). The bottom surface morphology analysis confirms that the interpenetrating structure is preserved at the gate interface in the thermally stable high-performance blends (fig. S3).

To elucidate the observed thermal stability of the 60 wt % PVK blend versus pure P1, we use in situ temperature-dependent UV-Vis spectroscopy, AFM, and grazing incidence x-ray diffraction (GIXD), as well as molecular dynamics simulations to study the effect of temperature on the intermolecular interactions of the semiconducting chains. Upon heating, the UV-Vis absorption spectra of pristine P1 films revealed a blue shift of 35 nm in the maximum absorption peak, accompanied by a decrease in both the 0-0 and the 0-1 peaks (Fig. 2A). These phenomena are consistent with the polymer chains' deaggregating and reorganizing caused by the thermal energy disrupting the crystallites. For the blend films, the chain ordering and interchain interactions were less affected upon heating, in comparison with pristine P1 films, as evidenced by the less pronounced decrease of the 0-0 vibronic peak intensity. More distinctively, the 0-0 vibronic peak that vanished in the P1 films was retained in the blended films even at temperatures up to 220°C (Fig. 2B). The temperature-dependent AFM analysis also revealed that the microscale morphology of the pristine P1 films changes upon heating, whereas the P1/PVK blend film morphology is not affected by heating (fig. S4). Together, these observations indicated that the matrix polymer effectively confined the semiconducting polymer and limited dihedral twisting and larger structural reorganizations that were responsible for the loss of the carrier mobility at high temperatures.

In situ temperature-dependent GIXD studies showed that in the 60% PVK blend film, the  $\pi$ - $\pi$  stacking distance of P1 was reduced from 3.70 to 3.64 Å, relative to the pristine P1 (Fig. 2, C and D, and fig. S5). In both cases, the  $\pi$ - $\pi$  stacking distance increased when the thin films were heated and reached 3.79 and 3.73 Å at 200°C for the pure P1 and the PVK blend films, respectively.

<sup>1</sup>Department of Chemistry, Purdue University, 560 Oval Drive, West Lafayette, IN 47907, USA. <sup>2</sup>Department of Physical & Biological Sciences-Chemistry and Biochemistry, University of California Santa Cruz, 1156 High Street, Santa Cruz, CA 95064, USA. <sup>3</sup>SLAC National Accelerator Laboratory, Stanford University, 2575 Sand Hill Road, Menlo Park, CA 94025, USA. <sup>4</sup>Charles D. Davidson School of Chemical Engineering, 480 Stadium Mall Drive, Purdue University, West Lafayette, IN 47906, USA.

\*Corresponding author. Email: bsavoie@purdue.edu (B.M.S.); jgmei@purdue.edu (J.M.)



To evaluate the effect of this  $\pi$ - $\pi$  stacking confinement on the polymer dihedral distribution, molecular dynamics modeling was performed. In these simulations, the  $\pi$ - $\pi$  separation of the semiconducting polymer chains was restrained to model varying levels of confinement, and the resulting dihedral distributions were compared to characterize the polymer reorganization dynamics (Fig. 2E). At  $\pi$ - $\pi$  confinements of 3.0 Å, we observed complete conservation of the dihedral distributions at all temperatures. Notably, the CCCN dihedral, corresponding to the DPP-T conformations, exhibited interconversion between gauche conformers, but there was no evidence of gauche-to-trans interconversion (i.e., the onset of chain twisting) at any temperature. Likewise, the SCCC dihedral angle, corresponding to the thiophene-thiophene conformations, broadened with temperature but remained sharply peaked. By contrast, at  $\pi$ - $\pi$  confinements of 5.0 Å, the SCCC dihedral distribution is broadened at all temperatures, and the CCCN dihedral exhibits gauche-to-trans interconversion at all temperatures (Fig. 2, F and G). Systematic studies of the dihedral distributions under confinements from 3 to 6 Å allowed us to conclude that large-scale DPP-T reorganizations began relatively abruptly once fluctuations in the interchain  $\pi$ - $\pi$  separation reach  $\sim$ 5 Å (figs. S7 to S9). On the basis of these results, we in-

terpret the  $\pi$ - $\pi$  confinement exhibited by the bicontinuous P1/PVK blends to play a critical role in restricting intrachain reorganization and enabling temperature-insensitive mobility. This mechanism suggests that this confinement strategy should be general to other semiconducting polymers embedded in similarly rigid matrix polymers or potentially to other confinement strategies like channel templating. The relatively broad range of blending concentrations that exhibit temperature insensitivity (40 to 70%) implies that this effect is relatively insensitive to the width of the confined semiconducting domains.

To evaluate the stability of the blend films under prolonged thermal stress, the fabricated FET devices were subjected to constant heating at 150°C for 6 hours in air. For inorganic semiconductors, prolonged heating leads to increased charge-carrier density and uncontrolled thermal doping (23). For organics, prolonged heating, especially above the  $T_g$  or the melting point of the semiconductors, leads to morphology changes and device performance degradation (10, 11, 15). In contrast with the pristine P1 devices under the same conditions, the devices based on the 60% PVK blends retained excellent electronic properties (as high as 95% of the original mobility) under thermal stress (Fig. 3A). The FET devices made from pristine P1 showed a declining on-off current ratio

( $I_{ON}/I_{OFF}$ ) and increased threshold voltages under constant heating, consistent with earlier observation of unstable morphologies at high temperatures. The thermally stabilized blend-based FET devices retain an on-off current ratio higher than  $10^3$  and threshold voltages below 3 V after thermal stressing (Fig. 3, B to D).

To demonstrate the generality of our blending strategy, we explore the FET thermal stability of P1 blended with four other high- $T_g$  matrices i.e., polycarbonate (PC), polyaceneaphthylene (PAC), polyetherimide (PEI), and Matrimid 5218 (MI) (Fig. 4A). We first optimized the blending ratios to attain interpenetrating morphologies (fig. S10A). FET devices based on these optimized blends exhibited thermally stable charge transport and the P1/PAC blend pair could reach hole mobilities as high as 2.0 cm<sup>2</sup>/V·s that were stable up to 220°C in open air (Fig. 4B). The optimized P1/PC blend only provided thermally stable operation up to 180°C, which is near the  $T_g$  of the host. We also tested other donor-acceptor semiconductors based on high-performance DPP (P2) (20) and isoindigo (P3) (24) (Fig. 4C) and studied the thermal stability of their blend films with the champion high- $T_g$  matrices, i.e., PVK and PAC. After optimizing the blend ratios to obtain an interpenetrating morphology (fig. S10B), FET devices with excellent thermal stability up to 220°C were also achieved

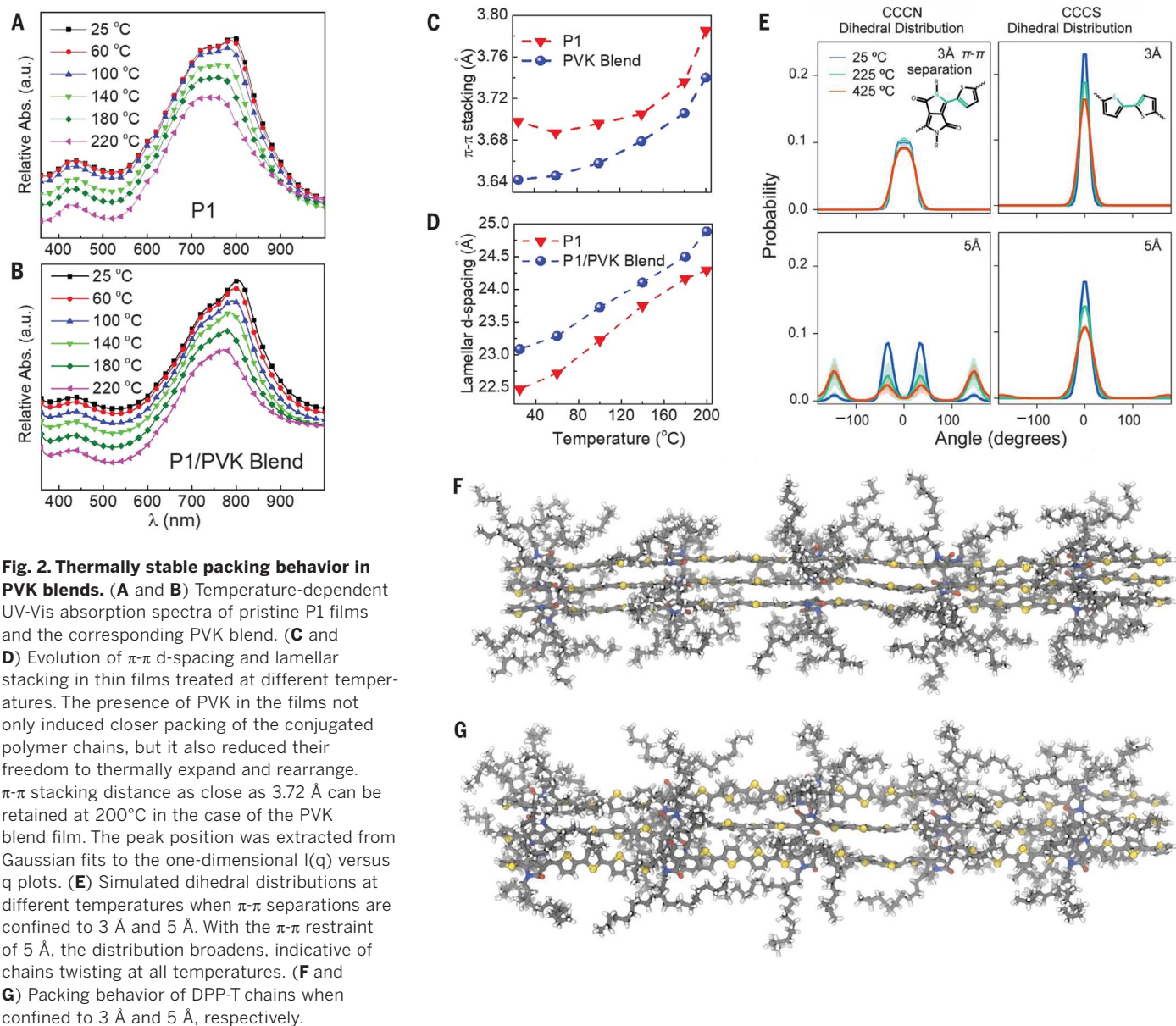


**Fig. 2. Thermally stable packing behavior in PVK blends.** (A and B) Temperature-dependent UV-Vis absorption spectra of pristine P1 films and the corresponding PVK blend. (C and D) Evolution of  $\pi$ - $\pi$  d-spacing and lamellar stacking in thin films treated at different temperatures. The presence of PVK in the films not only induced closer packing of the conjugated polymer chains, but it also reduced their freedom to thermally expand and rearrange.  $\pi$ - $\pi$  stacking distance as close as 3.72 Å can be retained at 200°C in the case of the PVK blend film. The peak position was extracted from Gaussian fits to the one-dimensional  $I(q)$  versus  $q$  plots. (E) Simulated dihedral distributions at different temperatures when  $\pi$ - $\pi$  separations are confined to 3 Å and 5 Å. With the  $\pi$ - $\pi$  restraint of 5 Å, the distribution broadens, indicative of chains twisting at all temperatures. (F and G) Packing behavior of DPP-T chains when confined to 3 Å and 5 Å, respectively.

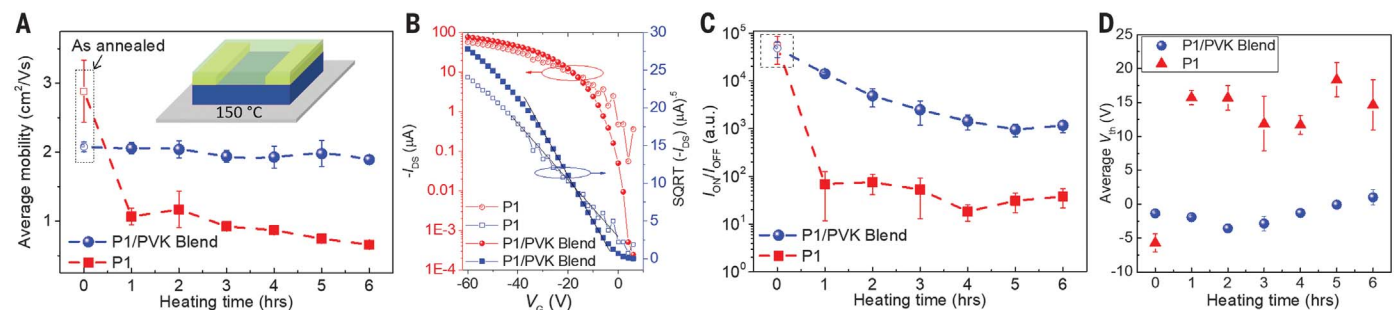


**Fig. 3. Effect of thermal stress on FET devices and thermal stability of PVK blends.** (A) Measured hole mobilities under constant thermal stress for 6 hours. A sudden decline in mobility was observed for pure P1 when the FET device is heated. The blend can retain its original mobility after 6 hours. (B) Characteristic transfer curves of FET devices based on P1 with and without PVK after 1 hour of heating. SQRT, square root.

(C) Impact of heating on the  $I_{ON}/I_{OFF}$ . After 1 hour of heating, the ratio fell to nearly 10 for the devices based on P1 while remaining  $> 10^4$  for the blend devices. (D) Threshold voltages ( $V_{th}$ ) for FET devices based on the 60% PVK blends (below 3 V) and pure P1 (exceeding 20 V) upon prolonged heating. The data points represent the average values measured from 10 different devices, and the error bars represent the standard deviation from the average.

#### Fig. 4. Attaining universal thermal stability in semiconducting polymer blends.

(A) Molecular structures and glass-transition temperatures of the representative matrix polymers tested for high-temperature charge transport. Matrimid 5218; PEI, polyetherimide. (B) Hole mobilities of FET devices based on the optimized blends of P1 in four different matrices measured in open air. (C) Molecular structures of additional semiconducting polymers studied for thermally stable blends. (D) Measured FET mobilities from the blend films of P2 and P3 with PVK and PAC used as the host matrices. The blend combinations that had stable close packing exhibited hole mobilities stable up to 220°C. The data points represent the average mobility values measured from 10 different devices, and the error bars represent the standard deviation from the average.

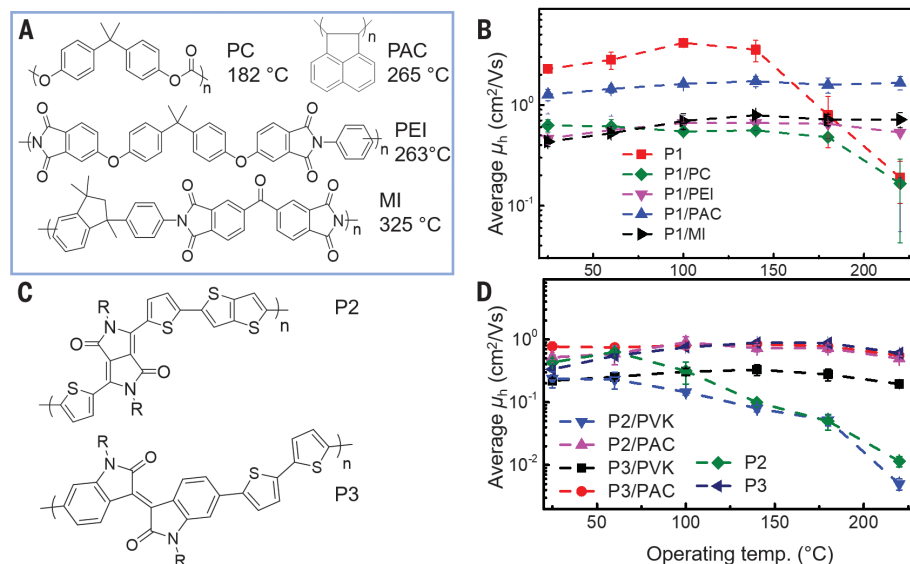


(Fig. 4D). Temperature-dependent UV-Vis absorption analyses on the blend films of P2 and P3 confirmed that those blend pairs with thermally insensitive charge transport properties exhibited a similar behavior as the P1/PVK blend at high temperatures (figs. S11 to S14). One exception was the P2/PVK pair, which did not present a thermally stable charge transport behavior (Fig. 4D). Likewise, this pair did not preserve the characteristic intermolecular interaction vibronic peak upon heating, indicating that this was a necessary feature in stable blends (fig. S12). We also noticed that the pristine P3 film exhibited a nearly thermally stable operation across the tested temperature range. Consistent with the thermally stable blends previously discussed, the P3 film itself also exhibited strong intermolecular interactions even at high temperatures (fig. S13), which suggested the organization of P3 is unusually robust among the studied semiconductors. Lastly, the blending strategy was tested for n-type semiconducting systems, and the blend films that form interpenetrating morphologies exhibited thermally stable operation in comparison with the pristine thin films (fig. S20).

To design high-temperature semiconducting polymer blends, a few requirements appear to be essential: (i) a host matrix with a  $T_g$  higher than the desired operating temperature; (ii) a semicrystalline semiconducting polymer; (iii) the interpenetration of the semiconducting component into the host matrix; and (iv) improved intermolecular  $\pi$ - $\pi$  stacking within semiconducting channels that can be retained at high temperature. The use of high- $T_g$  matrices is demonstrated

to be a general strategy to attain these properties by minimizing spatial rearrangements within the polymer films at elevated temperatures. We hypothesized that the superior ordering in the confined channels enhanced charge transport by reduced activation energy and trap density.

#### REFERENCES AND NOTES

- P. G. Neudeck, R. S. Okojie, L.-Y. Chen, *Proc. IEEE* **90**, 1065–1076 (2002).
- S. M. Sze, in *Physics of Semiconductor Devices*, K. K. Ng, Ed. (Wiley-Interscience, ed. 3, 2007).
- J. Watson, G. Castro, *J. Mater. Sci. Mater. Electron.* **26**, 9226–9235 (2015).
- T. P. Chow, R. Tyagi, *IEEE Trans. Electron Dev.* **41**, 1481–1483 (1994).
- P. G. Neudeck *et al.*, *IEEE Electron Device Lett.* **29**, 456–459 (2008).
- B. Hunt, A. Tooke, in *Proceedings of the 18th European Microelectronics Packaging Conference* (IEEE, 2011), pp. 1–5.
- G. Horowitz, *Adv. Mater.* **10**, 365–377 (1998).
- H. Sirringhaus *et al.*, *Nature* **401**, 685–688 (1999).
- V. Coropceanu *et al.*, *Chem. Rev.* **107**, 926–952 (2007).
- Y. Zhao *et al.*, *Adv. Mater.* **29**, 1605056 (2017).
- J. Chen *et al.*, *J. Polym. Sci., B, Polym. Phys.* **44**, 3631–3641 (2006).
- H. Sirringhaus, *Adv. Mater.* **26**, 1319–1335 (2014).
- T. Sekitani, S. Iba, Y. Kato, T. Someya, *Appl. Phys. Lett.* **85**, 3902–3904 (2004).
- J. T. Kintigh *et al.*, *J. Phys. Chem. C* **118**, 26955–26963 (2014).
- M. Seifrid, M. J. Ford *Adv. Mater.* **29**, 1605511 (2017).
- S. Goffri *et al.*, *Nat. Mater.* **5**, 950–956 (2006).
- A. Kumar, M. A. *Adv. Mater.* **21**, 4447–4451 (2009).
- S.-Y. Min *et al.*, *Nat. Commun.* **4**, 1773 (2013).
- E. K. Lee, M. Y. Lee, C. H. Park, H. R. Lee, J. H. Oh, *Adv. Mater.* **29**, 1703638 (2017).
- Y. Lei *et al.*, *Adv. Mater.* **28**, 6687–6694 (2016).
- Y. Lei *et al.*, *Sci. Rep.* **6**, 24476 (2016).
- F. C. Spano, C. Silva, *Annu. Rev. Phys. Chem.* **65**, 477–500 (2014).

23. W. Wondrak, *Microelectron. Reliab.* **39**, 1113–1120 (1999).

24. R. Stalder, J. Mei, K. R. Graham, L. A. Estrada, J. R. Reynolds, *Chem. Mater.* **26**, 664–678 (2014).

#### ACKNOWLEDGMENTS

We thank the Stanford Synchrotron Radiation Laboratory (a national user facility operated by Stanford University on behalf of the U.S. Department of Energy, Office of Basic Energy Sciences, under contract no. DE-AC02-76SF00515) for providing the equipment for the GIXD measurements.

**Funding:** This work was supported by the Office of Naval Research Young Investigator Program (ONR YIP Award, no. N00014-16-1-2551) and the National Science Foundation (NSF CAREER Award, no. 1653909).

**Author contributions:** A.G. and J.M. designed the experiments; A.G. processed the thin films, did the morphology characterizations, and fabricated and characterized the transistor devices; D.T.T. and Y.Z. helped with the measurements under nitrogen. X.L. synthesized the conjugated polymers; D.T.T. performed the DSC measurements; K.A.J. helped with the UV-Vis measurements. G.M.P., T.J.D. and A.L.A. designed and performed the GIXD measurements. B.M.S. designed and performed all the computational work. A.G., B.M.S., and J.M. organized the data and wrote the manuscript, and all authors contributed to the editing of the manuscript. J.M. conceived and directed the project. **Competing interests:** A.G. and J.M. are inventors on a patent application no. 62677648 submitted by the Office of Technology Commercialization Purdue Research Foundation. **Data and materials availability:** All data needed to evaluate the conclusions in the manuscript are provided in the manuscript or the supplementary materials.

#### SUPPLEMENTARY MATERIALS

www.sciencemag.org/content/362/6419/1131/suppl/DC1  
Materials and Methods  
Tables S1 to S3  
Figs. S1 to S20  
References (25–33)

1 August 2018; accepted 29 October 2018  
10.1126/science.aau0759